GEOPHYSICAL RESEARCH LETTERS, VOL. 22, NO. 1, PAGES 21-24, JANUARY 1, 1995

Equations of state of α, ϵ and liquid iron and iron's melting curve — Thermodynamic calculations

Guangqing Chen and Thomas J. Ahrens

Lindhurst Laboratory of Experimental Geophysics
Seismological Laboratory, California Institute of Technology
Pasadena, California

Abstract. The melting curve between ϵ and liquid iron (100GPa< P <300GPa) has been derived by computing Gibbs free energies at high pressures and high temperatures from equations of state of the α, ϵ and liquid phases. The most uncertainty lies in the equation of state (EOS) of the ϵ phase. By comparing the calculations to experimental data, the internal thermodynamic consistency of the three phases are examined. The best fits to the melting curves of *Boehler* [1993] and *Williams et al.* [1987] can be obtained with lower bulk moduli than determined by static compression. Using available equations of state of the iron phases, our calculations indicate that if sub-solidus iron is of the ϵ phase, Boehler's melting curve is thermodynamically more consistent than Williams et al.'s. The problem is complicated by the possible existence of a new phase between the ϵ and the liquid fields.

Introduction

The melting curve under high pressures between ϵ and liquid iron is directly related to the inner core-outer core temperature of the Earth. However, major disagreements exist between results from static and shock-wave measurements [*Boehler*, 1993; *Williams et al.*, 1987]. In this paper we attempt to determine the melting curve from equations of state of the α, ϵ and liquid phases in a thermodynamically consistent manner. The benefit of this approach can be two-fold: (1) it may give preference to a certain melting curve; (2) it also highlights thermodynamic quantities which need to be better determined in order to further constraint the melting curve.

Gibbs Free Energy Calculation Within a Single Phase

Two approaches we used in calculating Gibbs free energy (G) of a single phase as a function of P and T are outlined below.

Paper number 94GL02892
0094-8534/95/94GL-02892$03.00

Calculation Using an Isotherm-Isobar Mesh

In this approach [*Song and Ahrens*, 1994], $G(P,T)$ is calculated from reference point $G(P_0,T_0)$ by moving along the isobar to (P_0,T) then the isotherm to (P,T):

$$G(P,T) = H(P_0,T) - TS(P_0,T) + \int_0^P V(T,P')dP' \quad (1)$$

where the first two terms are

$$H(P_0,T) = H(P_0,T_0) + \int_{T_0}^T C_p(P_0,T')dT' \quad (2)$$

$$S(P_0,T) = S(P_0,T_0) + \int_{T_0}^T \frac{C_p(P_0,T')}{T'}dT' \quad (3)$$

$H(P_0,T_0)$ and $S(P_0,T_0)$ are enthalpy and entropy of formation from elements, V and C_p are volume and specific heat at constant pressure.

For the last term on the right hand side of Eq. 1, $V(T,P')$ is again calculated on the P'-T mesh: First, $V(T_0,P')$ is calculated from, *e.g.*, third order Birch-Murnaghan equation-of-state

$$P' = \frac{3}{2}K_T\left[\left(\frac{V(P_0,T_0)}{V(P',T_0)}\right)^{7/3} - \left(\frac{V(P_0,T_0)}{V(P',T_0)}\right)^{5/3}\right] \times\left(1+\frac{3}{4}(K_T'-4)\left[\left(\frac{V(P_0,T_0)}{V(P',T_0)}\right)^{2/3}-1\right]\right) \quad (4)$$

given the reference volume, isothermal bulk modulus K_T and its derivative K_T', then it undergoes thermal expansion to the final state:

$$V(P',T) = V(P',T_0)\exp\left[\int_{T_0}^T \alpha(P',T')dT'\right] \quad (5)$$

The thermal expansion coefficient $\alpha(P',T')$ is usually experimentally determined only at P' =1bar. The pressure dependence assumed is:

$$\alpha(P',T') = \alpha(P_0,T')\left[\frac{V(P',T')}{V(P_0,T')}\right]^{\delta} \quad (6)$$

where δ is the second Grüneisen parameter which is taken to be constant.

Gibbs energies of the α and ϵ phases of iron are calculated with this method.

Calculation Using an Isentrope-Isometric Mesh

The calculation of the Gibbs energy of liquid iron employs:

$$G(P,T) = E(P,T) - TS(P,T) + PV(P,T) \quad (7)$$

At any P and T, E, S and V are calculated by first moving along an isentrope from (P_0, T_0) to (P_s, T_s), at which the internal energy is E_s and volume is V_s:

$$E_s(P_s) = E(P_0,T_0) - \int_{V_0}^{V_s} P_s dV \quad (8)$$

$$T_s(P_s) = T_0 \exp\left[-\int_{V_0}^{V_s} \left(\frac{\gamma}{V}\right) dV\right] \quad (9)$$

where V_s is again determined by third order Birch-Murnaphan EOS (same as Eq. 4 with isothermal bulk modulus and its pressure derivative substituted with their isentropic conterparts). γ is the Grüneisen parameter, for liquid iron, it has been fit as a function of internal energy, *i.e.*, in Eq. 9, $\gamma = \gamma(E_s)$.

The second step is to move along an isometric to (P,T). With $V(P,T)$ held at constant V_s, either P or T are variable. We treat the final pressure P as a free parameter, therefore $T = T(P, P_s)$. The internal energy of the final state (E) is given by solving the Mie-Grüneisen equation:

$$\int_{E_s}^{E} \gamma(E')dE' = V_s(P - P_s) \quad (10)$$

then the following equation is solved for T:

$$\int_{T_s}^{T} C_v(T', V_s)dT' = E - E_s \quad (11)$$

and S is

$$S = S_0 + \int_{T_s}^{T} \frac{C_v(T', V_s)}{T'} dT' \quad (12)$$

Eqs. 10–12 give all the thermodynamic quantities needed to evaluate Eq. 7, given values for K_s, K_s', C_v and γ.

Gibbs Energy of α and Liquid Iron

Huang et al. [1987] reported α iron high-pressure compression data with the reference state at 1bar and 300K. We used *Robie et al.* [1979]'s data for C_p.

For liquid iron, the reference state is at the melting point (1809K) at 1bar. H_0 and S_0 are calculated from the values of the α phase at the same pressure and temperature, and the enthalpy change upon melting. We used the EOS parameters of liquid iron in *Anderson and Ahrens* [1994a].

Gibbs Energy of ϵ Iron

K_T and K_T' for ϵ iron have been measured by X-ray diffraction under static compression [*Huang et al.*, 1987; *Mao et al.*, 1990]. Thermal expansion coefficient is poorly constrained, previous estimates from static experiments exist in the 150–450°C, 10–20GPa region ($\sim 3\text{–}5\times10^{-5}\text{K}^{-1}$ [*Huang et al.*, 1987]), shock wave data yield a mean value of α from 300 to ~5200K at 202GPa ($\sim 9 \times 10^{-6}\text{K}^{-1}$ [*Duffy and Ahrens*, 1993]). No experimental data is available for the specific heat. We calculated C_v by summing the contributions from the lattice (given by the Debye model) and from the electrons. For the electronic contribution (C_e), we adopted the theoretical results of *Boness et al.* [1986]. We assumed the following value for C_v:

$$C_v(P,T) = c\left[9R \times D\left(\frac{T_D}{T}\right) + C_e\right] \quad (13)$$

where D is the Debye function, and Debye temperature for ϵ iron is 385K [*Andrews*, 1973; *Kerley*, 1993]. c is an *ad hoc* parameter: if our model is correct, c is unity.

C_p is then calculated from C_v by

$$C_p = C_v + \alpha^2 V K_T T \quad (14)$$

The reference state is chosen to be (12GPa, 300K), at which the α phase transfers to ϵ. The entropy change of the transition ΔS at 300K is unknown, but from the Clausius-Claperon relation:

$$\Delta S = \Delta V \frac{dP}{dT} \quad (15)$$

(ΔV is the volume change during the α-γ phase change at 300K [*Huang et al.*, 1987], $\frac{dP}{dT}$ is the slope of the phase boundary in P-T plane (reviewed in [*Besson and Nicol*, 1990]), it is estimated the enthalpy change $\Delta H = T\Delta S$ is no more than $\sim$ 0.6kJ/mol, or about 5% of the enthalpy of iron melting under 1 bar. In absence of more accurate data, we set ΔH to zero in our calculations.

Melting Curve Between the ϵ and Liquid Phases

After the Gibbs energies of the ϵ and liquid phases are calculated independently, the melting curve is where the two Gibbs energy surfaces intersect. We keep the α and liquid phases EOS fixed and adjust the ϵ phase to fit experimentally determined melting curves [*Boehler*, 1993; *Williams et al.*, 1987].

In the following sections we discuss the effects of various parameters (C_p, K_T, α) of the ϵ phase which are not well determined from experiments.

Specific Heat

We vary C_p by changing the parameter c in Eq. 13. It has a pronounced effect on the slope of the $G_\epsilon(T)$ at a given pressure. The effect is nearly the same at different pressures (Figure 1(a)). At c=1 (the theoretical value),

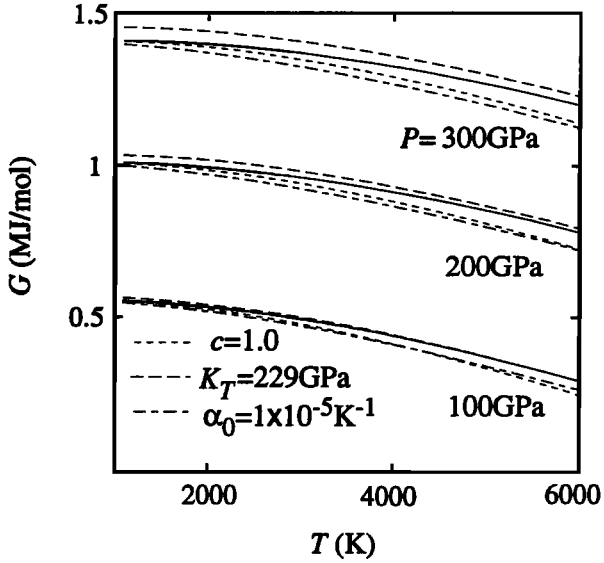

Figure 1. Effects of specific heat, bulk modulus and thermal expansion on G. Solid curve is for $c = 0.9, K_T = 190$GPa, K_T'=4, $\alpha_0 = 4 \times 10^{-5}$K^{-1},$\beta = 2 \times 10^{-5}$ and $\delta = 3.2$. Parameters changed for dashed curves are indicated.

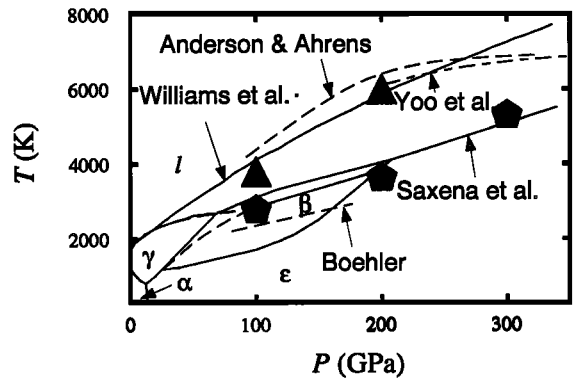

Figure 2. Iron phase diagrams given by different groups. Boehler's and Saxena's phase diagrams are similar except the β-ϵ boundary. The melting curves from shock wave data are all higher than static curves. The solid-solid transition on the principal Hugoniot at $\sim$ 200GPa observed by Brown and McQueen (not shown in graph) has a higher temperature than either Boehler or Saxena's β-ϵ transition temperature at that pressure. Filled symbols are numerical fits using EOS parameters in Table 1 for the ϵ phase.

$G_\epsilon(T)$ drops faster than $G_l(T)$ at higher pressures (200–300GPa) such that they may never intersect. This is in clear contradiction with experimental data.

Bulk Modulus

The bulk modulus controls the gradient of $G_\epsilon(P)$ at a certain temperature (the spacing between 100, 200 and 300GPa curves in G-T plane, Figure 1(b)). The effect decreases with T due to K_T's temperature dependence, so K_T also effects the slope of $G_\epsilon(T)$, though much less directly than C_p does. The effect can further be fine-tuned by K_T'.

Thermal Expansion

α has a similar effect on $G_\epsilon(P)$ at fixed pressures as C_p (smaller α gives steeper $G_\epsilon(P)$, Figure 1(c)), but the change of slope has much stronger pressure dependence than that caused by C_p. Again, the effect can be subtly controlled with α's temperature dependence ($\frac{1}{\alpha_0}(\frac{\partial \alpha}{\partial T})_P \equiv \beta$) and pressure dependence (δ).

P-T Phase Diagrams of Iron

Boehler [1993] and *Saxena et al.* [1993] suggested a relatively low melting curve (although they disagree about the stability region of the new β phase, see Figure 2). *Saxena et al.* [1994] proposed the phase diagram shown in Figure 2 based on their experimental data and thermodynamic calculations similar to ours. *Williams et al.* [1987], *Yoo et al.* [1993] approximately agreed on a higher melting curve obtained completely or partially (data from *Bass et al.* [1987] are incorporated in the Williams paper) from shock wave experiments. Recently *Anderson and Ahrens* [1994b] revised shock temperature calculations of *Bass et al.* [1987] which arrived at a lower melting point at high pressures (> 230GPa), but not enough to explain the difference between the static and shock wave data. The origin of the solid-solid transformation observed in the principal Hugoniot (at $\sim$ 200GPa [*Brown and McQueen*, 1986]) before melting (at $\sim$ 243GPa) is uncertain. Brown and McQueen interpreted it as the ϵ-γ transition, while *Boehler* [1993] believed it is between ϵ and β. *Anderson* [1994] offered a third scenario by suggesting yet another solid phase θ above 200GPa and 4000K. Structure studies of the β phase are only theoretical. *Matsui* [1992] suggested it is bcc from his molecular simulation work, but *Stixrude and Cohen* [1994] concluded bcc structure is unstable in the $\sim$ 150GPa range from density function theory. It is almost certain there is at least one phase between the ϵ and liquid stability fields in the pressure range of 100–300GPa, but the equation of state of the phase is unknown and hence calculating its fusion curve is infeasible.

Conclusions

Fits to *Boehler* [1993] and *Williams et al.* [1987]'s data are obtained (Figure 2) using two sets of parameters listed in Table 1. Notice the parameters are cen-

Table 1. EOS parameters used for ϵ-iron to fit experimental melting curves

	K_T(GPa)	K_T'
Boehler	205	4.8
Williams	120	7.5

Reference state is 12GPa and 300K. Other paramters (common to both fits) are $c = 0.90$, $\alpha = 3 \times 10^{-5}$K^{-1}, $\beta = 2 \times 10^{-5}$ and $\delta = 3.2$.

tered at 12GPa, 300K. Extrapolated to ambient conditions, K_T^0 (bulk modulus at 1bar and 300K) used to fit Boehler's data is 147GPa, significantly lower than the 204GPa (with K_T'=5) reported by *Huang et al.* [1987]. The 147GPa value is closer to *Mao et al.* [1990]'s data (165GPa). Mao's data, however, yields a melting curve too low in the 100–300GPa range. Interestingly, the values of $K_T^0 \simeq$ 30GPa and K_T'=7.5 are necessary to fit Williams et al.'s data. Therefore, assuming the phase diagram and the equations of state of the α and liquid phases are approximately correct, our calculations favor Boehler's melting curve over Williams'. Finally, in either fit, the specific heat is 10% lower than its theoretical value.

Although we cannot completely delineate the effects of all variables on the Gibbs energy of the ϵ phase, we note that to fit Williams' data, the bulk modulus must be lowered to fit the melting point at 100GPa (~4000K). Although steepening the Gibbs energy temperature dependence (by, e.g., increasing the value of C_p) would also raise the M. P. at 100GPa, it yields too high a M. P. at 200GPa. More experimental data on the β and ϵ (especially its thermal expansion coefficient) would lead to more definite conclusions from our calculations.

Acknowledgments. Research supported by NSF. We thank William Anderson for helpful discussions. Contribution # 5433, Division of Geology and Planetary Sciences, California Institute of Technology.

References

Anderson, O. L., Imperfections of the 1993 phase diagram of iron, in *High Pressure Science and Technology-1993*, edited by S. C. Schmidt, J. W. Shaner, G. A. Samara, and M. Ross, pp. 907-910, American Institute of Physics Press, New York, 1994.

Anderson, W. W., and T. J. Ahrens, An equation of state for liquid iron and implications for the Earth's core, *J. Geophys. Res., 99,* 4273-4284, 1994a.

Anderson, W. W., and T. J. Ahrens, Shock temperatures and melting in iron sulfides at core pressures, *J. Geophys. Res.*, 1994b, submitted.

Andrews, D. J., Equation of state of the alpha and epsilon phases of iron, *J. Phys. Chem. Solids, 34,* 825-840, 1973.

Bass, J. D., B. Svendsen, and T. J. Ahrens, The temperatures of shock-compressed iron, in *High Pressure Res. in Mineral Physics*, edited by M. Manghnani and Y. Syono, pp. 393-402, Terra, Tokyo, 1987.

Besson, J. M., and M. Nicol, An equation of state of γ-Fe and some insights about magnetoelastic effects on measurements of the α-γ-ϵ triple point and other transitions, *J. Geophys. Res., 95,* 21717-21720, 1990.

Boehler, R., Temperatures in the Earth's core from melting-point measurements of iron at high static pressures, *Nature, 363,* 534-536, 1993.

Boness, D. A., J. M. Brown, and A. K. McMahan, The electronic thermodynamics of iron under Earth core conditions, *Phys. Earth Planet. Inter., 42,* 227-240, 1986.

Brown, J. M. and R. G. McQueen, Phase transitions, Grüneisen parameter, and elasticity for shocked iron between 77GPa and 400GPa, *J. Geophys. Res., 91,* 7485-7494, 1986.

Duffy, T. S., and T. J. Ahrens, Thermal expansion of mantle and core materials at very high pressures, *Geophys. Res. Lett., 20,* 1103-1106, 1993.

Huang, E., W. A. Bassett, and P. Tao, Pressure-temperature-volume relationship for hexagonal close packed iron determined by synchrotron radiation, *J. Geophys. Res., 92,*, 8129-8135, 1987.

Kerley, G. I., Multiphase Equation of State for Iron, *Sandia Report,* SAND93-0027, 1993.

Mao, H. K., Y. Wu, L. C. Chen, J. F. Shu, and A. P. Jephcoat, Static compression of iron to 300GPa and $Fe_{0.8}Ni_{0.2}$ alloy to 260GPa: Implications for composition of the core, *J. Geophys. Res., 95,* 21737-21742, 1990.

Matsui, M., Computer simulation of the structural and physical properties of iron under ultra high pressures and high temperatures, *Central Core of the Earth, 2,* 79-82, 1992.

Robie, R. A., B. S. Hemingway, and J. R. Fisher, Thermodynamic Properties of Minerals and related Substances at 298.15K and 1 Bar (10^5 Pascals) Pressure and at Higher Temperatures, *U. S. Geol. Survey Bull.*, 1452, 1979.

Saxena, S. K., G. Shen and P. Lazor, Experimental evidence for a new iron phase and implications for Earth's core, *Science, 260,* 1312-1314, 1993.

Saxena, S. K., G. Shen and P. Lazor, Temperatures in Earth's core based on melting and phase transformation experiments on iron, *Science, 264,* 405-407, 1994.

Song, X., and T. J. Ahrens, Pressure-temperature range of reactions between liquid iron in the outer core and mantle silicates, *Geophys. Res. Lett., 21,* 153-156, 1994.

Stixrude, L., and R. E. Cohen, Constraints on the crystalline structure of the inner core: Mechanical instability of bcc iron at high pressure, *Geophys. Res. Lett.*, in press.

Williams, Q., R. Jeanloz, J. Bass, B. Svendsen, and T. J. Ahrens, The melting curve of iron to 250 gigapascals: A constraint on the temperature at the Earth's center, *Science, 236,* 181-182, 1987.

Yoo, C. S., N. C. Holmes, M. Ross, D. J. Webb, and C. Pike, Shock temperatures and melting of iron at Earth core conditions, *Phys. Rev. Lett., 70,* 3931-3934, 1993.

G. Chen and T. J. Ahrens, 252-21, California Institute of Technology, Pasadena, CA 91125 (e-mail: guang@earth.gps.caltech.edu, tja@earth.gps.caltech.edu).

(received October 17, 1994;
accepted November 1, 1994.)